Report on Near-optimal dynamic trajectory generation and control of an omnidirectional vehicle

Neha Madhekar (UID: 119374436)
Yashas Shetty (UID: 119376348)

1 Abstract

Usually optimal control leads to computationally costly solutions. Whereas on the other hand a cheap solution may lead to an unstable control. There are many applications in which precise optimal control is not necessary and rather computational speed is required. This paper presents a novel technique to calculate a control input which generates a near optimal trajectory for an omni-directional vehicle based system. This control input is generated at a significantly lower cost as well.

The complex non-linear system has been linearized by restricting the admissible controls. By applying a simple constraint on the control input, a near optimal trajectory is generated. As the computational cost of this strategy is low, a beneficial trade off between cost and optimality is achieved.

2 Introduction

Having the capability to move in any direction irrespective of the rotation, makes the omnidirectional drive very advantageous while manoeuvring in dynamic environments. A prominent use-case of omnidirectional vehicles is in warehouse applications where this omnidirectional motion makes navigation optimal. Path planning also becomes easier. Hence use of omnidirectional drives is very much favourable in robotic applications.

The authors refer to [10,13] saying that most papers on trajectory control of omnidirectional vehicles have dealt with relatively static environments.Here, the trajectory control is essentially performed by first building a geometric path and then by using feedback control to track the path. This stratergy is effective when collision free path is more important than time optimality. However, the dynamic capabilities of the vehicle play an important role in fast paced enivronments. Authors have given references to many path planning techniques used previously . They mention the techniques used by Muñoz et al. [14] , Fiorini and Shiller [8] , Faiz and Agrawal [6] , Watanabe et al. [20], Tanaka et

al. [18].
This paper deals with near-optimal dynamic trajectory generation and control of an omnidirectional vehicle. The first section of the paper provides an abstract on the paper. Following that, an introduction to the topic is given in the second section. In the third section of this paper the authors derive kinematic and dynamic model of a three wheeled omnidirectional vehicle which will be used in the later sections. The non linear control problem is then linearized in the fourth section by restricting admissible controls.In the fifth section, the control input for the optimal trajectory is calculated and the control input for the near optimal trajectory (similar to that of that bang bang trajectory) is also generated. The near optimal trajectory is then simulated in the sixth section and compared to the optimal trajectory. The last section, provides a conclusion on the results obtained from the previous section. Following the conclusion there is an appendix and list of the references used in the paper.

3 Kinematic and dynamic modeling of the omnidirectional vehicle

The omnidirectional drive (also known as holonomic drive) facilitates the robot to move in any direction without rotation. This type of drive system is very useful in robotics. This research study is done for 3 wheeled omni drive. This drive consists of 3 sets of wheel assemblies equally spaced at 120 degrees from one another as shown in the figure below. Each assembly has omni wheel, gearbox and actuator (motor) attached to it. The omni wheels not only roll forward like normal wheels, but also slide sideways with almost no friction due to the orthogonal rollers used. The point of symmetry of the three wheels is assumed to be coincident with Centre of mass of the robot.

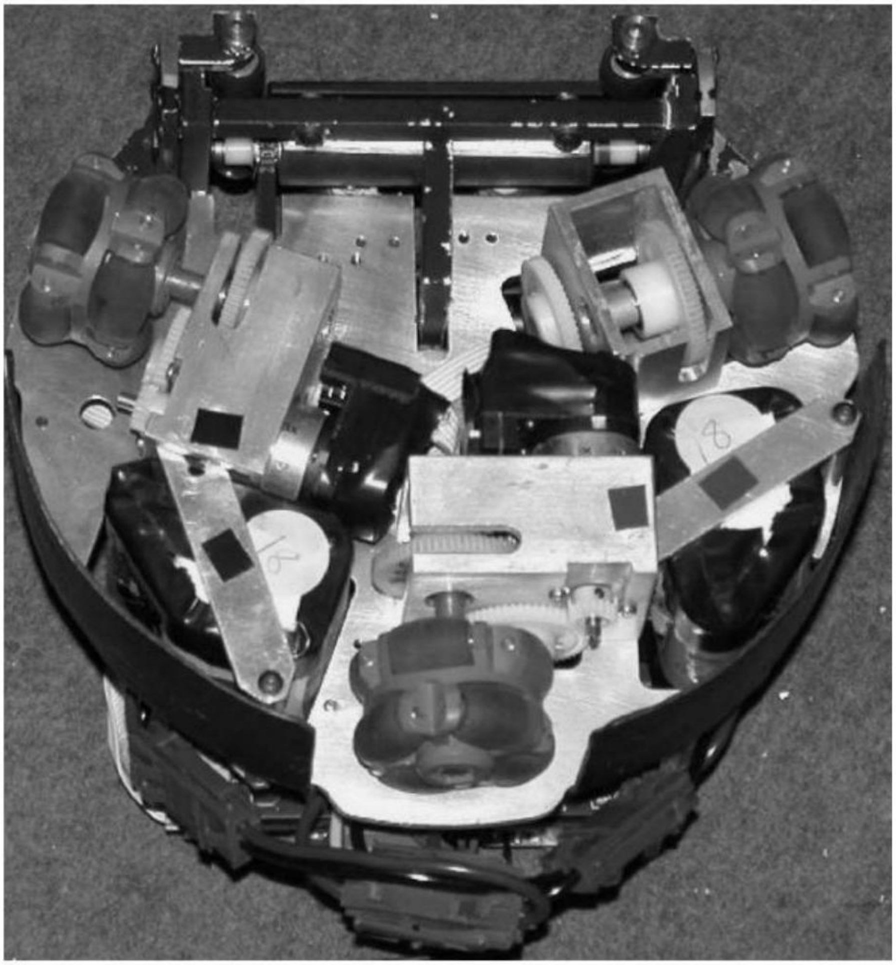

Fig. 1. Bottom view of the omnidirectional vehicle.

3.1 Vehicle kinematics

The omnidirectional robot has 3 degrees of freedom in a plane viz. translation along x axis, translation along y axis, and rotation about z axis (normal to the plane). The schematic diagram of the vehicle is given below.

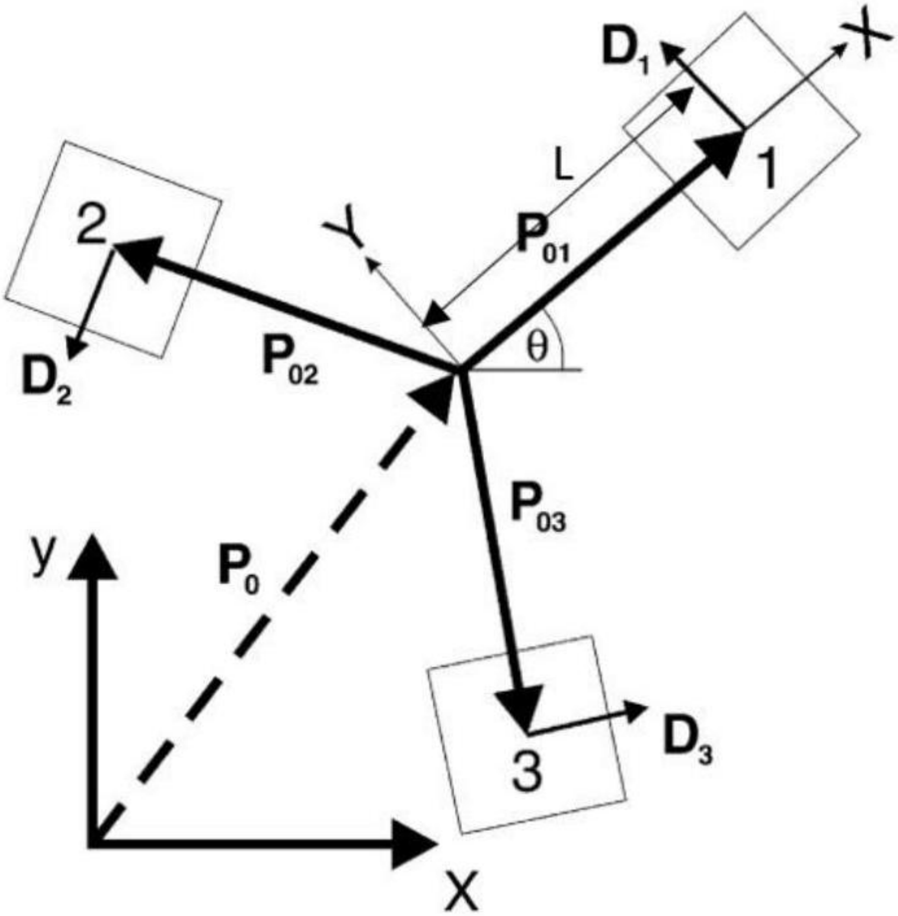

Fig. 2. Geometry of the omnidirectional vehicle.

Let P_0 be the position of the centre of mass of the robot. Then the positions P_{0i} of all wheel assemblies with respect to the centre of mass of the robot can be simply represented as the rotation about z axis.

Let L be the distance between centre of mass of the robot and wheel assembly.

The position of first wheel assembly is given by,

$$P_{01} = L \begin{bmatrix} 1 \\ 0 \end{bmatrix} \tag{1}$$

The rotation about z-axis is given by the matrix $R(\theta)$ where θ is measured positive anticlockwise.

$$R(\theta) = \begin{bmatrix} \cos(\theta) & -\sin(\theta) \\ \sin(\theta) & \cos(\theta) \end{bmatrix} \tag{2}$$

For getting the position of the second wheel assembly, P_{01} is rotated anticlockwise by 120 degrees about z axis.

$$P_{02} = R\left(\frac{2\pi}{3}\right) P_{01} = \mathrm{L}\begin{bmatrix} \cos\left(\frac{2\pi}{3}\right) & -\sin\left(\frac{2\pi}{3}\right) \\ \sin\left(\frac{2\pi}{3}\right) & \cos\left(\frac{2\pi}{3}\right) \end{bmatrix}\begin{bmatrix} 1 \\ 0 \end{bmatrix} = \frac{L}{2}\begin{bmatrix} -1 \\ \sqrt{3} \end{bmatrix} \tag{3}$$

Similarly, the position of the third wheel assembly can be derived by rotating P_{01} anticlockwise by 240 degrees or by rotating P_{02} anticlockwise by 120 degrees.

$P_{03} = R\left(\frac{4\pi}{3}\right) P_{01} = \mathrm{L}\begin{bmatrix} \cos\left(\frac{4\pi}{3}\right) & -\sin\left(\frac{4\pi}{3}\right) \\ \sin\left(\frac{4\pi}{3}\right) & \cos\left(\frac{4\pi}{3}\right) \end{bmatrix}\begin{bmatrix} 1 \\ 0 \end{bmatrix} = \frac{-\mathrm{L}}{2}\begin{bmatrix} 1 \\ \sqrt{3} \end{bmatrix}$
or

$$P_{03} = R\left(\frac{2\pi}{3}\right) P_{02} = \frac{L}{2}\begin{bmatrix} \cos\left(\frac{2\pi}{3}\right) & -\sin\left(\frac{2\pi}{3}\right) \\ \sin\left(\frac{2\pi}{3}\right) & \cos\left(\frac{2\pi}{3}\right) \end{bmatrix}\begin{bmatrix} -1 \\ \sqrt{3} \end{bmatrix} = \frac{-\mathrm{L}}{2}\begin{bmatrix} 1 \\ \sqrt{3} \end{bmatrix} \tag{4}$$

As shown in fig. 2, the unit vector D_i specifies the drive direction of each wheel relative to the centre of mass of the robot. D_i is perpendicular to the position vector P_{0i}. Therefore, we will get the direction of D_i by rotating $\mathrm{P}_{0\mathrm{i}}$ vector by 90 degrees. For a unit vector, we need to divide by magnitude of P_{0i} vector i.e., L.

$$\mathrm{D_i} = \frac{1}{\mathrm{L}} R\left(\frac{\pi}{2}\right) P_{0\mathrm{i}} = \frac{1}{\mathrm{L}}\begin{bmatrix} \cos\left(\frac{\pi}{2}\right) & -\sin\left(\frac{\pi}{2}\right) \\ \sin\left(\frac{\pi}{2}\right) & \cos\left(\frac{\pi}{2}\right) \end{bmatrix} P_{0\mathrm{i}} = \frac{1}{\mathrm{L}}\begin{bmatrix} 0 & -1 \\ 1 & 0 \end{bmatrix} P_{0\mathrm{i}} \tag{5}$$

From the above equation, D_1, D_2 and D_3 are computed.

$$\begin{gathered} \mathrm{D}_1 = \frac{1}{\mathrm{L}}\begin{bmatrix} 0 & -1 \\ 1 & 0 \end{bmatrix} L \begin{bmatrix} 1 \\ 0 \end{bmatrix} = \begin{bmatrix} 0 \\ 1 \end{bmatrix} \\ \mathrm{D}_2 = \frac{1}{\mathrm{L}}\begin{bmatrix} 0 & -1 \\ 1 & 0 \end{bmatrix} \frac{\mathrm{L}}{2}\begin{bmatrix} -1 \\ \sqrt{3} \end{bmatrix} = -\frac{1}{2}\begin{bmatrix} \sqrt{3} \\ 1 \end{bmatrix} \\ \mathrm{D}_3 = \frac{1}{\mathrm{L}}\begin{bmatrix} 0 & -1 \\ 1 & 0 \end{bmatrix} \frac{-\mathrm{L}}{2}\begin{bmatrix} 1 \\ \sqrt{3} \end{bmatrix} = \frac{1}{2}\begin{bmatrix} \sqrt{3} \\ -1 \end{bmatrix} \end{gathered} \tag{6}$$

3.2 The motor characteristics

In general, the optimal control problem for independent actuator driven wheels is treated with either bounded velocity or bounded acceleration but not both. In our case we follow this because for a DC motor, the shaft torque and angular velocity are dependent on each other. The model

$$\mathrm{T} = \bar{\alpha}\mathrm{U} - \bar{\beta}\omega \tag{7}$$

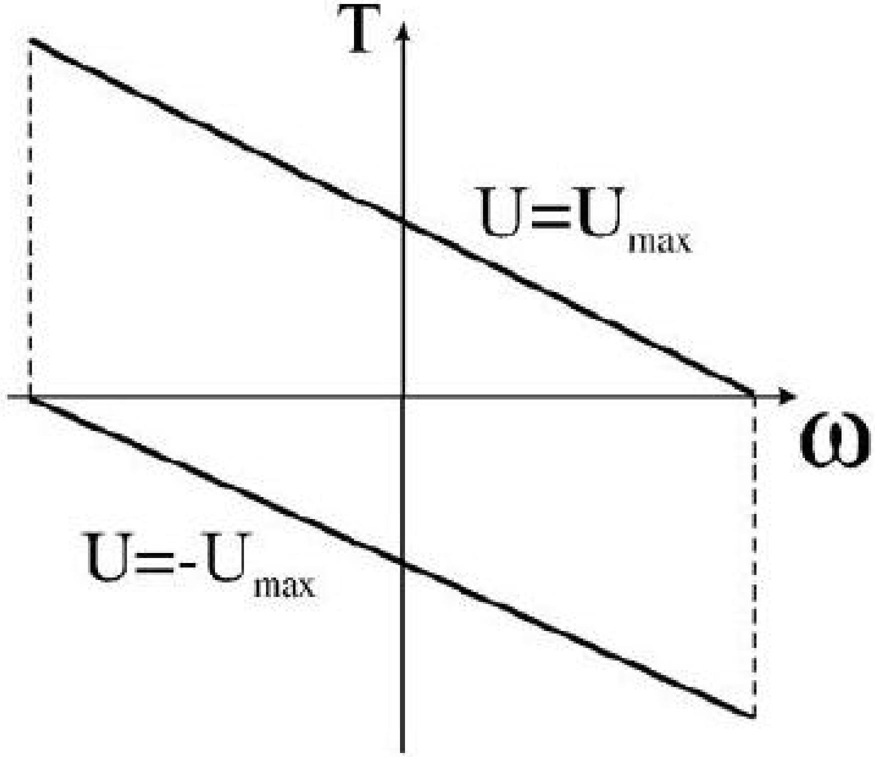

Fig. 3. Torque-speed characteristics of a DC motor.

Models the torque output based on input voltage(U) and shaft angular velocity(ω) pretty accurately. As L is very small, it is neglected for this equation. The constants $\bar{\alpha}$ (N m/V) and $\bar{\beta}$(N m s) are characteristic to the motor. With the no-slip condition, the force generated by a DC motor driven wheel is simply

$$\mathrm{f} = \alpha \mathrm{U} - \beta v \tag{8}$$

where $f(N)$ is the magnitude of the force generated by a wheel attached to the motor, and v(m/s) is the velocity of the wheel. The constants α(N/V) and β(kg/s) can readily be determined from $\bar{\alpha}$, $\bar{\beta}$, and the geometry of the vehicle.

4 Equations of motion

The centre of mass of the robot is represented by the position P_0 and rotation θ with respect to fixed frame.

$$P_0 = \begin{bmatrix} x \\ y \end{bmatrix} \tag{9}$$

The positions of the wheel assemblies w.r.t. fixed frame is given by,

$$\mathrm{r_i} = P_0 + R(\theta)P_{0\mathrm{i}} \tag{10}$$

We will get the velocities at drive positions by differentiating the above equation with respect to time.

$$\mathrm{v_i} = \dot{P}_0 + \dot{R}(\theta)P_{0\mathrm{i}} \tag{11}$$

The individual wheel velocity is

$$v_\mathrm{i} = \mathrm{v_i^T} R(\theta)\mathrm{D_i} \tag{12}$$

From equation 11 ,

$$\begin{aligned} \mathrm{v_i^T} &= \left(\dot{P}_0 + \dot{R}(\theta)P_{0\mathrm{i}}\right)^\mathrm{T} \\ &= \dot{P}_0^\mathrm{T} + P_{0\mathrm{i}}^\mathrm{T}\dot{R}^\mathrm{T}(\theta) \end{aligned} \tag{13}$$

Therefore, substituting equation (11) in equation (12) ,

$$\begin{aligned} v_\mathrm{i} &= \left(\dot{P}_0^\mathrm{T} + P_{0\mathrm{i}}^\mathrm{T}\dot{R}^\mathrm{T}(\theta)\right) R(\theta)\mathrm{D_i} \\ v_\mathrm{i} &= \dot{\mathrm{P}}_0^\mathrm{T} R(\theta)\mathrm{D_i} + \mathrm{P}_{0\mathrm{i}}^\mathrm{T}\dot{R}^\mathrm{T}(\theta)R(\theta)\mathrm{D_i} \end{aligned} \tag{14}$$

The second term of the right-hand side is just the tangential velocity.

$$\mathrm{P_{0i}}^\mathrm{T}\dot{R}^\mathrm{T}(\theta)R(\theta)\mathrm{D_i} = \mathrm{L}\dot{\theta} \tag{15}$$

Hence,

$$\begin{aligned} v_\mathrm{i} &= \dot{\mathrm{P}}_0^\mathrm{T} R(\theta)\mathrm{D_i} + \mathrm{L}\dot{\theta} \\ v_\mathrm{i} &= \begin{bmatrix} \dot{\mathrm{x}} & \dot{\mathrm{y}} \end{bmatrix} \begin{bmatrix} \cos(\theta) & -\sin(\theta) \\ \sin(\theta) & \cos(\theta) \end{bmatrix} \mathrm{D_i} + \mathrm{L}\dot{\theta} \\ v_\mathrm{i} &= \begin{bmatrix} \dot{\mathrm{x}}\cos(\theta) + \dot{\mathrm{y}}\sin(\theta) & -\dot{\mathrm{x}}\sin(\theta) + \dot{\mathrm{y}}\cos(\theta) \end{bmatrix} \mathrm{D_i} + \mathrm{L}\dot{\theta} \end{aligned} \tag{16}$$

Let's find the velocities of all wheels.

$$
\begin{aligned}
v_1 &= [\dot{\mathrm{x}}\cos(\theta) + \dot{\mathrm{y}}\sin(\theta) - \dot{\mathrm{x}}\sin(\theta) + \dot{\mathrm{y}}\cos(\theta)]\mathrm{D}_1 + \mathrm{L}\dot{\theta}\\
v_1 &= [\dot{\mathrm{x}}\cos(\theta) + \dot{\mathrm{y}}\sin(\theta) \quad - \dot{\mathrm{x}}\sin(\theta) + \dot{\mathrm{y}}\cos(\theta)]\begin{bmatrix} 0 \\ 1 \end{bmatrix} + L\dot{\theta}\\
v_1 &= -\dot{\mathrm{x}}\sin(\theta) + \dot{\mathrm{y}}\cos(\theta) + \mathrm{L}\dot{\theta}\\
v_2 &= [\dot{\mathrm{x}}\cos(\theta) + \dot{\mathrm{y}}\sin(\theta) - \dot{\mathrm{x}}\sin(\theta) + \dot{\mathrm{y}}\cos(\theta)]\mathrm{D}_2 + \mathrm{L}\dot{\theta}\\
v_2 &= [\dot{x}\cos(\theta) + \dot{y}\sin(\theta) \quad - \dot{x}\sin(\theta) + \dot{\mathrm{y}}\cos(\theta)]\begin{bmatrix} -\sqrt{3} \\ 2 \\ \frac{-1}{2} \end{bmatrix} + \mathrm{L}\dot{\theta} \tag{17}\\
v_2 &= -\sin\left(\frac{\pi}{3} - \theta\right)\dot{\mathrm{x}} - \cos\left(\frac{\pi}{3} - \theta\right)\dot{\mathrm{y}} + \mathrm{L}\dot{\theta}\\
v_3 &= [\dot{\mathrm{x}}\cos(\theta) + \dot{\mathrm{y}}\sin(\theta) - \dot{\mathrm{x}}\sin(\theta) + \dot{\mathrm{y}}\cos(\theta)]\mathrm{D}_3 + \mathrm{L}\dot{\theta}\\
v_3 &= [\dot{\mathrm{x}}\cos(\theta) + \dot{\mathrm{y}}\sin(\theta) \quad - \dot{\mathrm{x}}\sin(\theta) + \dot{\mathrm{y}}\cos(\theta)]\begin{bmatrix} \frac{\sqrt{3}}{2} \\ \frac{-1}{2} \end{bmatrix} + \mathrm{L}\dot{\theta}
\end{aligned}
$$

$$
v_3 = \sin\left(\frac{\pi}{3} + \theta\right)\dot{\mathrm{x}} - \cos\left(\frac{\pi}{3} + \theta\right)\dot{\mathrm{y}} + \mathrm{L}\dot{\theta} \tag{18}
$$

Writing above equations in matrix form,

$$
\begin{bmatrix} v_1 \\ v_2 \\ v_3 \end{bmatrix} = \begin{bmatrix} -\sin(\theta) & \cos(\theta) & \mathrm{L} \\ -\sin\left(\frac{\pi}{3} - \theta\right) & -\cos\left(\frac{\pi}{3} - \theta\right) & \mathrm{L} \\ \sin\left(\frac{\pi}{3} + \theta\right) & -\cos\left(\frac{\pi}{3} + \theta\right) & \mathrm{L} \end{bmatrix} \begin{bmatrix} \dot{\mathrm{x}} \\ \dot{\mathrm{y}} \\ \dot{\theta} \end{bmatrix} \tag{19}
$$

Applying the linear and angular momentum balance:

$$
\begin{gathered}
\sum_{\mathrm{i}=1}^{3} \mathrm{f_i} R(\theta)\mathrm{D_i} = \mathrm{m}\ddot{P}_0\\
\mathrm{L}\sum_{\mathrm{i}=1}^{3} \mathrm{f_i} = \mathrm{J}\ddot{\theta}
\end{gathered} \tag{20}
$$

where f_i is the magnitude of the force produced by the i^{th} motor, m is the mass of the robot and J is the moment of inertia of the robot.

Using (8) together with the balance laws of (20) and replacing the v_i' s from the kinematic relation (14) results,

$$
\begin{gathered}
\sum_{\mathrm{i}=1}^{3} \left(\alpha \mathrm{U_i} - \beta v_{\mathrm{i}}\right) R(\theta)\mathrm{D_i} = \mathrm{m}\ddot{P}_0\\
\mathrm{L}\sum_{\mathrm{i}=1}^{3} \left(\alpha \mathrm{U_i} - \beta v_{\mathrm{i}}\right) = \mathrm{J}\ddot{\theta}
\end{gathered} \tag{21}
$$

This system of differential equations can be expressed as

$$\begin{bmatrix} \mathrm{m}\ddot{\mathrm{x}} \\ \mathrm{m}\ddot{\mathrm{y}} \\ \mathrm{J}\ddot{\theta} \end{bmatrix} = \alpha\widehat{\mathrm{P}}(\theta)\mathrm{U}(\mathrm{t}) - \frac{3\beta}{2}\begin{bmatrix} \dot{\mathrm{x}} \\ \dot{\mathrm{y}} \\ 2\ \mathrm{L}^2\dot{\theta} \end{bmatrix} \tag{22}$$

with

$$\widehat{\mathrm{P}}(\theta) = \begin{bmatrix} -\sin(\theta) & -\sin\left(\frac{\pi}{3}-\theta\right) & \sin\left(\frac{\pi}{3}+\theta\right) \\ \cos(\theta) & -\cos\left(\frac{\pi}{3}-\theta\right) & -\cos\left(\frac{\pi}{3}+\theta\right) \\ \mathrm{L} & \mathrm{L} & \mathrm{L} \end{bmatrix} \text{ and}$$

$$\mathrm{U}(\mathrm{t}) = \begin{bmatrix} \mathrm{U}_1(\mathrm{t}) \\ \mathrm{U}_2(\mathrm{t}) \\ \mathrm{U}_3(\mathrm{t}) \end{bmatrix} \tag{23}$$

The author has introduced the new time and length scales as

$$\mathrm{T} = \frac{2\ \mathrm{m}}{3\beta}, \quad \psi = \frac{4\alpha\mathrm{m}\mathrm{U}_{\mathrm{max}}}{9\beta^2}, \quad \Theta = \frac{4\alpha\mathrm{m}^2\mathrm{L}\mathrm{U}_{\mathrm{max}}}{9\ \mathrm{J}\beta^2} \tag{24}$$

and the new non-dimensional variables become

$$\overline{\mathrm{x}} = \frac{\mathrm{x}}{\psi}, \quad \overline{\mathrm{y}} = \frac{\mathrm{y}}{\psi}, \quad \bar{\theta} = \frac{\theta}{\Theta}, \quad \bar{\mathrm{t}} = \frac{\mathrm{t}}{\mathrm{T}}, \quad \overline{\mathrm{U}}_{\mathrm{i}}(\mathrm{t}) = \frac{\mathrm{U}_{\mathrm{i}}(\mathrm{t})}{\mathrm{U}_{\mathrm{max}}} \tag{25}$$

The non-dimensional equations of motion (after dropping the bars) become

$$\begin{bmatrix} \ddot{x} \\ \ddot{y} \\ \ddot{\theta} \end{bmatrix} + \begin{bmatrix} \dot{x} \\ \dot{y} \\ \frac{2\ \mathrm{mL}^2}{J}\dot{\theta} \end{bmatrix} = q(\theta, t) \tag{26}$$

where $q(\theta, t)$ is the control action

$$q(\theta, t) = P(\theta)U(t) \tag{27}$$

with

$$\mathrm{P}(\theta) = \begin{bmatrix} -\sin(\theta) & -\sin\left(\frac{\pi}{3}-\theta\right) & \sin\left(\frac{\pi}{3}+\theta\right) \\ \cos(\theta) & -\cos\left(\frac{\pi}{3}-\theta\right) & -\cos\left(\frac{\pi}{3}+\theta\right) \\ 1 & 1 & 1 \end{bmatrix}$$

5 Restricting admissible controls

It is required to specify the three voltages $U_{\mathrm{i}}(\mathrm{t})$ to all three motors in order to move the robot. The authors state that the real time optimal control of the differential equation of the system is not feasible with modest computational resources. The complexity is due to non-linearity of the problem. The attempt is made to linearize the system. In this section, the authors aim to find a simplified, computationally tractable optimal control problem whose solution yields feasible, albeit sub-optimal, trajectories. This will be achieved by restricting the set of admissible controls. The set of feasible voltages U is a cube given by.

$$\mathrm{u}(\mathrm{t}) = \{\mathrm{U}(\mathrm{t}) \| \mathrm{U}_{\mathrm{i}}(\mathrm{t}) \mid \leq 1\} \tag{28}$$

The set of admissible controls $P(\theta)U(t)$ depends on the vehicle orientation θ. For simplifying the problem, the authors have replaced this set with θ-independent controls.

The maximal such set is found by taking the intersection of all possible sets of allowable controls.

$$\mathrm{Q(t)} = \bigcap_{\theta\epsilon[0,2\pi)} \mathrm{P}(\theta)\mathrm{u(t)} \tag{29}$$

Obviously, any $q(t) \in Q$ is a suitable replacement for the θ-dependent control action. The explicit representation of Q is given below.

$P(\theta)$ can be decomposed into

$$\mathrm{P}(\theta) = \mathrm{R_z}(\theta)\mathrm{P}(0) \tag{30}$$

where

$$\begin{aligned} \mathrm{R_z}(\theta) &= \begin{bmatrix} \cos(\theta) & -\sin(\theta) & 0 \\ \sin(\theta) & \cos(\theta) & 0 \\ 0 & 0 & 1 \end{bmatrix} \\ \mathrm{P}(0) &= \frac{1}{2}\begin{bmatrix} 0 & -\sqrt{3} & \sqrt{3} \\ 2 & -1 & -1 \\ 2 & 2 & 2 \end{bmatrix} \end{aligned} \tag{31}$$

The authors suggest that the linear transformation $P(0)$ maps the cube $U(t)$ into the tilted cuboid $P(0)U(t)$ with a diagonal $|q_\theta| \leq 3$ along the q_θ axis (Fig. 4).

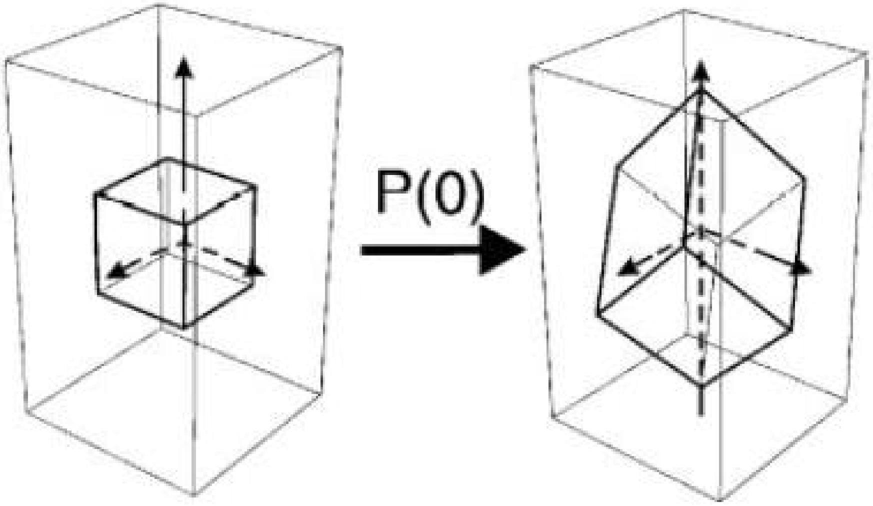

Fig. 4. The mapping $\mathbf{P}(0)$.

The transformation $R_z(\theta)$ then rotates this cuboid about the q_θ axis (or equivalently: about its diagonal). The solid of revolution that is the intersection of all possible rotations $R_z(\theta)P(0)U(t)$ of the cuboid is then the restricted admissible set of control.

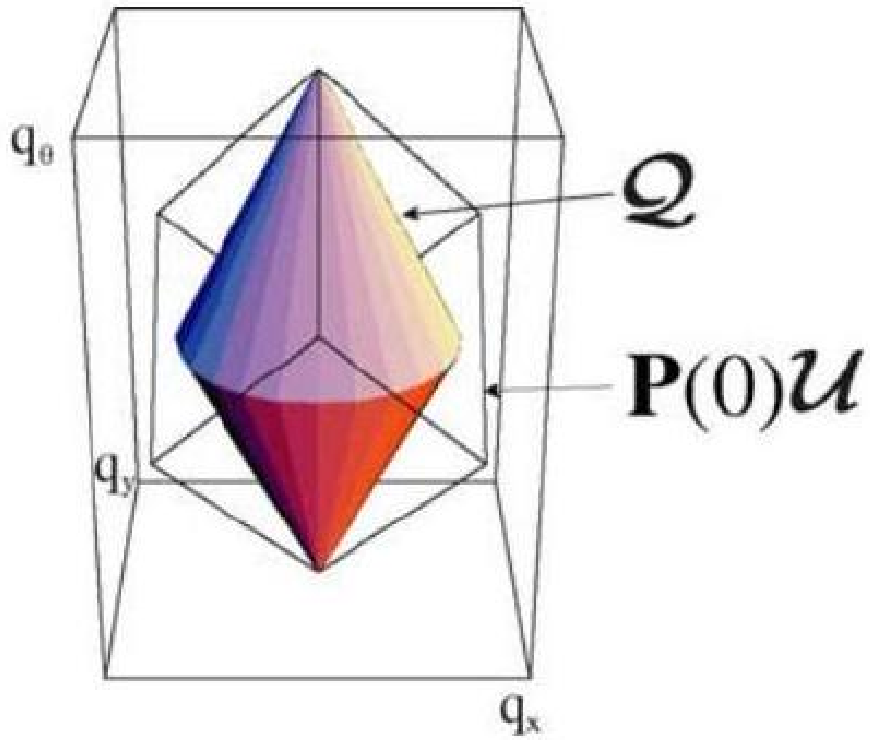

Fig. 5. Restricted set for admissible controls.
This solid of revolution is characterized by (see Appendix A for details)

$$\mathrm{q}_\mathrm{x}^2(\mathrm{t}) + \mathrm{q}_\mathrm{y}^2(\mathrm{t}) \leq \mathrm{r}^2\left(\mathrm{q}_\theta(\mathrm{t})\right) \tag{32}$$

where the radius is

$$r\left(\mathrm{q}_\theta(\mathrm{t})\right) = \frac{3 - |\mathrm{q}_\theta(\mathrm{t})|}{2} \tag{33}$$

To verify this, we plotted the vertices of cube and transformed each vertex by $P(0)$.

The vertices of the cube representing the set of feasible voltages would be $(-1,-1,-1), (-1,1,-1), (1,1,-1), (1,-1,-1), (1,1,1), (1,-1,1), (-1,1,1), (-1,-1,1)$.

The vertices of tilted cuboid after $P(0)$ transformation look like,

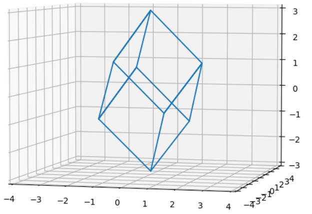

We then rotated the cuboid about the q_θ axis by applying transformation $R_z(\theta)$ and plotted it after every 10 degrees rotation.

The intersection of all the cuboids is deduced logically and highlighted in the right image shown below.

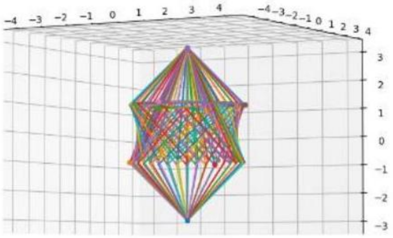

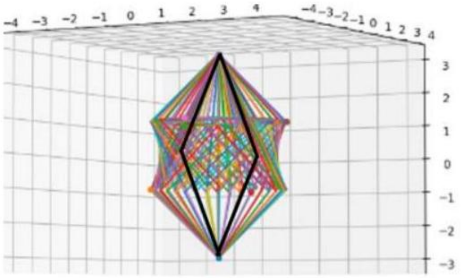

The solid of revolution is illustrated in Fig. 5, while its cross-section is shown in Fig. 6.

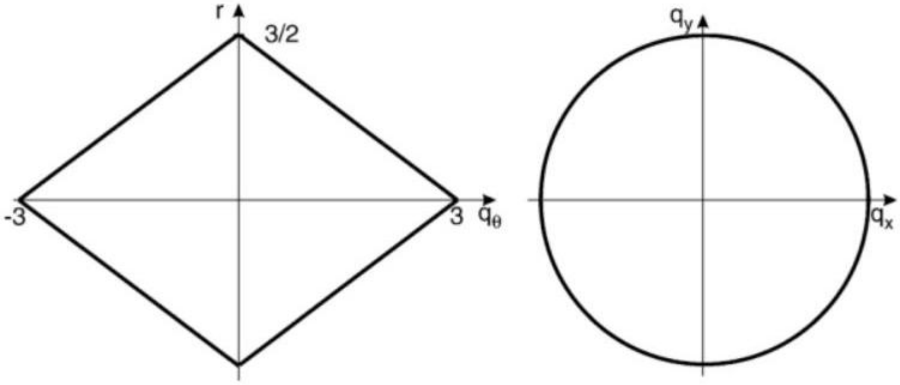

Fig. 6. Cross-section of the admissible set.

Using above results, equations of motion become

$$\begin{aligned}\ddot{\mathrm{x}} + \dot{\mathrm{x}} &= \mathrm{q_x(t)}\\ \ddot{\mathrm{y}} + \dot{\mathrm{y}} &= \mathrm{q_y(t)}\\ \ddot{\theta} + \frac{2\ \mathrm{mL}^2}{\mathrm{J}}\dot{\theta} &= \mathrm{q}_\theta\mathrm{(t)}\end{aligned} \tag{34}$$

These equations are now linear with the constraint on control effort.

$$\begin{aligned}&\mathrm{q_x^2(t)}{+}\mathrm{q_y^2(t)} \leq \left(\frac{3 - |\mathrm{q}_\theta\mathrm{(t)}|}{2}\right)^2\\ &|\mathrm{q}_\theta\mathrm{(t)}| \leq 3\end{aligned} \tag{35}$$

The authors have focused on controlling the translational DOFs in the remainder of the paper. It is assumed that the translational DOFs are controlled independently from the rotational DOF. There are two main reasons for this. First, it substantially simplifies the development of the results, and the results can readily be extended to encompass all three DOFs simultaneously. Second, the authors think that this paper will mainly be used for the applications where rotation control is independent of translational ones.

To decouple the θ-equation from those of the translational ones, the authors have set

$$|\mathrm{q}_\theta\mathrm{(t)}| \leq 1$$

Then the constraint for x and y becomes

$$q_x^2(t) + q_y^2(t) \leq 1 \tag{36}$$

6 Trajectory Generation

In this section, the authors solve equations for x, y and their respective velocities v_x and v_y (or $\dot{x}$ and $\dot{y}$)

Earlier , we have established that,

$$q_x(t) = \dot{x} + \ddot{x} \tag{37}$$

$$q_y(t) = \dot{y} + \ddot{y} \tag{38}$$

with the boundary conditions

$x(0) = 0, \quad x(t_f) = x_f, \quad \dot{x}(0) = v_{x0}, \quad \dot{x}(t_f) = 0$

$y(0) = 0, \quad y(t_f) = y_f, \quad \dot{y}(0) = v_{y0}, \quad \dot{y}(t_f) = 0$

We also have derived constraints on $q_x(t)$ and $q_y(t)$,

$$q_x(t)^2 + q_y(t)^2 \leq 1 \tag{39}$$

The authors have considered initial position to be (0,0) as any position can be translated to this position, thus keeping generality intact. Also the authors assume velocity at t_f will be zero as specifying a non-zero final velocity together with a final position often leads to solutions that do not continuously depend on the boundary conditions, which is not a desirable property in most applications.

We need to note that first t_f is to be minimized and then it can be considered as a constant for solving the rest of the equations.

We can write the above equations as follows,
$\ddot{x} = q_x(t) - \dot{x}$
$\ddot{y} = q_y(t) - \dot{y}$

For convenience we will write,
$\dot{x} = \dot{x}$
$\ddot{x} = q_x(t) - \dot{x}$
$\dot{y} = \dot{y}$
$\ddot{y} = q_y(t) - \dot{y}$

The above equations can be represented as the general form for a finite-dimensional state-space representation for a system with input $q(t)$ and state variable $z(t)$:

$\dot{z}(t) = Az(t) + Bq(t)$

where we define the control input $q(t)$ as

$$q(t) = \begin{bmatrix} q_x(t) \\ q_y(t) \\ 0 \\ 0 \end{bmatrix}$$

and state variable $z(t)$ as ,

$$z(t) = \begin{bmatrix} x(t) \\ \dot{x}(t) \\ y(t) \\ \dot{y}(t) \end{bmatrix}$$

thus we have $\dot{z}(t)$,

$$\dot{z}(t) = \begin{bmatrix} \dot{x}(t) \\ \ddot{x}(t) \\ \dot{y}(t) \\ \ddot{y}(t) \end{bmatrix}$$

And we can write

$$\dot{z}(t) = Az(t) + Bq(t) \tag{40}$$

with,

$$A = \begin{bmatrix} 0 & 1 & 0 & 0 \\ 0 & -1 & 0 & 0 \\ 0 & 0 & 0 & 0 \\ 0 & 0 & 0 & -1 \end{bmatrix}, \quad B = \begin{bmatrix} 0 & 0 & 0 & 0 \\ 1 & 0 & 0 & 0 \\ 0 & 0 & 0 & 0 \\ 0 & 1 & 0 & 0 \end{bmatrix} \tag{41}$$

And thus the boundary conditions for this system will be

$$z(0) = \begin{bmatrix} 0 \\ v_{x0} \\ 0 \\ v_{y0} \end{bmatrix}, \quad z(t_f) = \begin{bmatrix} x_f \\ 0 \\ y_f \\ 0 \end{bmatrix} \tag{42}$$

and subject to the conditions

$q_x(t)^2 + q_y(t)^2 \leq 1$

6.1 Minimum time trajectory

We know that the control input q is proportional to the input voltage to the motors, and for a DC motor, input voltage is proportional to the RPM of the motor. Hence to reach the final point in minimum time, we have to have q as large as possible

Thus for

$q_x(t)^2 + q_y(t)^2 \leq 1$

We take,

$$q_x^2(t) + q_y^2(t) = 1, \quad t \in [0, t_\text{f}]\,. \tag{43}$$

6.1.1 Time-Optimal control hypothesis:

The authors have stated the method to find time optimal control as follows,

The time-optimal control is given by ($\|\cdot\|$ denotes the Euclidean norm)

$$\mathbf{q}(t) = -\frac{B^{\mathrm{T}}\mathbf{p}(t)}{\|B^{\mathrm{T}}\mathbf{p}(t)\|}, \tag{44}$$

where $\mathbf{p}(t)$ is the solution to the adjoint problem

$$\dot{\mathbf{p}}(t) = -A^{\mathrm{T}}\mathbf{p}(t). \tag{45}$$

The two components of the time-optimal control are thus

$$q_x(t) = \frac{\lambda_1 + \mathrm{e}^{t-t_\mathrm{f}}(\lambda_2 - \lambda_1)}{\sqrt{\left(\lambda_1 + \mathrm{e}^{t-t_\mathrm{f}}(\lambda_2 - \lambda_1)\right)^2 + \left(\lambda_3 + \mathrm{e}^{t-t_\mathrm{f}}(\lambda_4 - \lambda_3)\right)^2}}, \tag{46}$$

$$q_y(t) = \frac{\lambda_3 + \mathrm{e}^{t-t_\mathrm{f}}(\lambda_4 - \lambda_3)}{\sqrt{\left(\lambda_1 + \mathrm{e}^{t-t_\mathrm{f}}(\lambda_2 - \lambda_1)\right)^2 + \left(\lambda_3 + \mathrm{e}^{t-t_\mathrm{f}}(\lambda_4 - \lambda_3)\right)^2}}, \tag{47}$$

where the parameters λ_i, t_f can be determined from the boundary conditions (37) and (38). The solution to system (41) and (42) is

$$\mathbf{z}(t) = \mathrm{e}^{At}\mathbf{z}(0) + \int_0^t \mathrm{e}^{A(t-\tau)}B\mathbf{q}(\tau)\mathrm{d}\tau \tag{48}$$

with this, the boundary conditions are written as (note that the initial conditions are automatically satisfied)

$$x_\mathrm{f} = v_{x0}\left(1 - \mathrm{e}^{-t_\mathrm{f}}\right) + \int_0^{t_\mathrm{f}} \left(1 - \mathrm{e}^{\tau - t_\mathrm{f}}\right) q_x(\tau)\mathrm{d}\tau \tag{49}$$

$$0 = \mathrm{e}^{-t_\mathrm{f}}v_{x0} + \int_0^{t_\mathrm{f}} \mathrm{e}^{\tau - t_\mathrm{f}} q_x(\tau)\mathrm{d}\tau \tag{50}$$

$$y_\mathrm{f} = v_{y0}\left(1 - \mathrm{e}^{-t_\mathrm{f}}\right) + \int_0^{t_\mathrm{f}} \left(1 - \mathrm{e}^{\tau - t_\mathrm{f}}\right) q_y(\tau)\mathrm{d}\tau \tag{51}$$

$$0 = \mathrm{e}^{-t_\mathrm{f}}v_{y0} + \int_0^{t_\mathrm{f}} \mathrm{e}^{\tau - t_\mathrm{f}} q_y(\tau)\mathrm{d}\tau. \tag{52}$$

An additional equation can be obtained from the fact that the Hamiltonian of the system (see [2]) is zero on $[0,\ t_\mathrm{f}\ ]$

$$H = 1 + (A\mathbf{z}(t) + B\mathbf{q}(t), \mathbf{p}(t)) = 1 - \lambda_2 q_x(t_\mathrm{f}) - \lambda_4 q_y(t_\mathrm{f}) = 0 \tag{53}$$

where $(\cdot, \cdot)$ denotes scalar product. This is equivalent to

$$\lambda_2^2 + \lambda_4^2 = 1. \tag{54}$$

The authors also state that resulting equations for q are quite complicated and for solving these equations, we need the numerical values of the λ_i for computing the integral equations . They could not find a computationally efficient method of solving this problem, both in the literature and using standard optimization packages thus making the problem computationally costly.

6.1.2 Anomaly in Time-Optimal control hypothesis:

As per For solving q, we try to find p. From equation 45, we can see that
$p = ke^{A^T t}$
Since A is a 4X4 matrix, p comes out to be 4X4 . Hence when calculate q, B and p are 4X4 matrices and norm is just a numerical value Hence we get q to be 4X4 as well

But as per the system definition, q is a 4X1 matrix.

6.1.3 The near Optimal control solution:

The authors then provide a constraint on $q(t)$ which makes it computationally very cheap. Further, the accuracy of the results with this constraint is compared with the optimal control output.

The constraint provided by the author is as follows,

$$|q_x(t)| = constant, \quad |q_y(t)| = constant \tag{55}$$

which means,

$$q_z(t) = q_z, \quad for \quad 0 < t \le t_1 \tag{56}$$

$$q_z(t) = -q_z, \quad for \quad t_1 < t \le t_f \tag{57}$$

where z represents either x or y

6.2 Bang–bang trajectory

The authors state that the minimum time problem i.e. finding minimum of t_f with a boundary value constraint problem always has a solution, and that the control which minimizes the final time t_f consists of two piecewise constant segments of magnitude 1. This type of control strategy is commonly referred to as “bang–bang” control. They reference Koh and Cho [12] where a path tracking problem for a two-wheeled robot based on bang–bang control is formulated.

In our case, the following must be solved for q, $t_1$and t_2

$$\dot{z} + \ddot{z} = q_z, \quad for \quad 0 < t \le t_1 \tag{58}$$

$$\dot{z} + \ddot{z} = -q_z, \quad for \quad t_1 < t \le t_1 + t_2 \tag{59}$$

where,

$t_2 = t_f$ - t_1

and boundary conditions are

$z(0) = 0, \quad z(t_f) = z_f, \quad \dot{z}(0) = v_0, \quad \dot{z}(t_f) = 0$

Solving the above two differential equations and applying the boundary conditions, we get

$$z(t) = e^{-t}(q_z - v_0) + q_z(t-1) + v_0 \quad for \quad 0 < t \leq t_1 \tag{60}$$

$$z(t) = q_z(t_f - e^{t_f - t} - t + 1) + z_f \quad for \quad t_1 < t \leq t_f \tag{61}$$

and

$$v(t) = (v_0 - q_z)e^{-t} + q_z \quad for \quad 0 < t \leq t_1 \tag{62}$$

$$v(t) = (e^{t_f - t} - 1)q_z \quad for \quad t_1 < t \leq t_f \tag{63}$$

Now, since the path of the robot is a continuous one, position function and velocity function would be continuous at t_1. Hence we equate the above equations at t_1,

$$e^{-t_1}(q_z - v_0) + q_z(t_1 - 1) + v_0 = q_z(t_f - e^{t_f - t_1} - t_1 + 1) + z_f \tag{64}$$

i.e.

$$e^{-t_1}(q_z - v_0) + q_z(t_1 - 1) + v_0 = q_z(t_2 - e^{t_2} + 1) + z_f \tag{65}$$

and,

$$(v_0 - q_z)e^{-t_1} + q_z = (e^{t_f - t_1} - 1)q_z \tag{66}$$

i.e.

$$(v_0 - q_z)e^{-t_1} + q_z = (e^{t_2} - 1)q_z \tag{67}$$

Hence, we get

$$t_1 = t_2 - \frac{c}{q_z} \tag{68}$$

$$q_z \left(\mathrm{e}^{t_2}\right)^2 - 2q_z \mathrm{e}^{t_2} + (v_0 - q_z)\, \mathrm{e}^{c/q_z} = 0, \tag{69}$$

where $c = v_0 - z_\mathrm{f}$. The second equation can be solved as

$$\mathrm{e}^{t_2}_{1,2} = 1 \pm \operatorname{sgn}(q_z) \sqrt{D}, \tag{70}$$

where

$$D = 1 + \mathrm{e}^{c/q_z} \left(\frac{v_0}{q_z} - 1 \right). \tag{71}$$

We also require $t_1 \geq 0, t_2 \geq 0$ which we will then provide

$$t_2 = \ln(1 + \sqrt{D}). \tag{72}$$

The following inequalities should hold:

$$D \geq 0, \tag{73}$$

$$\sqrt{D} \geq \mathrm{e}^{c/q_z} - 1. \tag{74}$$

If $c/q_z \leq 0$ then (78) has to be true, that is

$$\mathrm{e}^{-c/q_z} - 1 \geq -\frac{v_0}{q_z}. \tag{75}$$

If $c/q_z \geq 0$ then

$$D \geq \left(\mathrm{e}^{c/q_z} - 1\right)^2 \tag{76}$$

should be satisfied, which is equivalent to

$$\mathrm{e}^{c/q_z} - 1 \leq \frac{v_0}{q_z}. \tag{77}$$

Multiplying (75) and (77) by c/q_z (and taking its sign into account) yields

$$\frac{c}{q_z}\left(\mathrm{e}^{|c/q_z} \mid -1\right) \leq \left|\frac{c}{q_z}\right| \frac{v_0}{q_z}, \tag{78}$$

which can be further simplified to

$$\operatorname{sgn}\frac{c}{q_z}\left(\mathrm{e}^{|c/q_z} \mid -1\right) \leq \frac{v_0}{q_z}. \tag{79}$$

The sign of the first segment (± 1) is thus given by

$$q_z = \operatorname{sgn}\left(v_0 - \operatorname{sgn}(c)\left(\mathrm{e}^{|c|} - 1\right)\right). \tag{80}$$

Once q_z, t_1 and t_2 are determined, $z(t)$ is given in (60). The execution time for this trajectory (using (68) and (72)) is

$$t_{\mathrm{f\,min}} := t_1 + t_2 = 2\ln(1+\sqrt{D}) - \frac{c}{q_z}. \tag{81}$$

6.3 Trajectory synchronization

From the above equations, we get value of t_f for x and y. For finding a solution to our inputs i.e. the boundary conditions, we need to have satisfy the condition $t_{fx} = t_{fy}$.

The authors have made a preposition that for a $t_f \geq t_{fmin}$, bang-bang trajectory exists with a reduced control input. Now, from the above equation of t_f we can see that t_f is inversely proportional to q_z. So we can say that as q_z decreases, t_f increases. The authors define a set of control inputs for which the bang bang trajectory holds and $t_f \geq t_{fmin}$ in the preposition as follows

Proposition 1. For all $t_{\mathrm{f}} \geq t_{\mathrm{f\,min}}$ there exists $a\bar{q} \in (0,1]$ such that

$$q_z = \bar{q}\,\mathrm{sgn}\left(\frac{v_0}{\bar{q}} - \mathrm{sgn}(c)\left(\mathrm{e}^{|c/\bar{q}}\mid -1\right)\right), \tag{82}$$

satisfies (58) and (59). Furthermore, the execution time is a continuous, strictly monotonously decreasing function of $\bar{q}$ with $\lim_{\bar{q}\to 0} t_{\mathrm{f}} \to \infty$ and $t_{\mathrm{f}}(\bar{q} = 1) = t_{\mathrm{f\,min}}$.

Thus for different values of q, we can find corresponding t_f from the above equation (number) we can say t_f is a function of q_z, z_f, v_{z0}. Thus for x, t_f is a function of q_x, x_f, v_{x0}. And correspondingly, for y, t_f is a function of q_y, y_f, v_{y0}.

Now we know that,

$$t_{fx}(x_f, v_{x0}, q_x) = t_{fy}(y_f, v_{y0}, q_y) \tag{83}$$

We also have the constraint,

$$q_x(t)^2 + q_y(t)^2 = 1 \tag{84}$$

thus we get,

$$t_{fx}(x_f, v_{x0}, q_x) = t_y(y_f, v_{y0}, \sqrt{1 - q_x^2}) \tag{85}$$

Hence we have a set of q_x and a q_y satisfying the above equation. We will be finding out the the value of this q_x while solving for the given inputs.This solution will also depend continuously on the boundary conditions (given in Appendix B) which ensures robustness to disturbances.

For finding the value of q_x, we have to note that $t_{fx}(x_f, v_{x0}, q_x)$ is a strictly monotonously decreasing function on $|q_x| \in| (0,1], t_y(y_f, v_{y0}, \sqrt{1 - q_x^2})$ is strictly monotonously increasing there and thus $[t_{fx}(x_f, v_{x0}, q_x) - t_y(y_f, v_{y0}, \sqrt{1 - q_x^2})]$ is strictly monotonously decreasing.

7 Numerical solutions and simulations

In this section, as per the boundary conditions x_0, y_0, x_f, y_f and the robot specifications (we take $\alpha = 1$ N/V and $\beta = 1$ kg/s), we calculate the values of the control input q and t_f. Also the time step to update the value of positon and velocity is taken to be d$t = 1/60 = 0.017$

For calculating q: We had previously mentioned that $[t_{fx}(x_f, v_{x0}, q_x) - t_y(y_f, v_{y0}, \sqrt{1 - q_x^2})]$ is strictly monotonously decreasing and we know that there is a q_x which satisfies $[t_{fx}(x_f, v_{x0}, q_x) = t_y(y_f, v_{y0}, \sqrt{1 - q_x^2})]$. Thus, we use the bisection algorithm over here on $|q_x \in| (0,1]$ to find the required q_x. Ideally, q_x should be such that $[t_{fx}(x_f, v_{x0}, q_x) - t_y(y_f, v_{y0}, \sqrt{1-q_x^2})] = 0$ but finding this value may require a lot of time. Hence a tolerance of small value is given such that $|t_{fx}(x_f, v_{x0}, q_x) - t_y(y_f, v_{y0}, \sqrt{1-q_x^2})| \leq tolerance$. For convenience the author has selected this value to be equal to dt

Once we get the values of q_x, q_y, we find the value of $t_f, t_1 and t_2$ Then we use the equations (numbers) to find the position and velocity of the robot and given time t

$$z(t) = e^{-t}(q_z - v_0) + q_z(t-1) + v_0 \quad for \quad 0 < t \leq t_1 \tag{86}$$

$$z(t) = q_z(t_f - e^{t_f - t} - t + 1) + z_f \quad for \quad t_1 < t \leq t_f \tag{87}$$

and

$$v(t) = (v_0 - q_z)e^{-t} + q_z \quad for \quad 0 < t \leq t_1 \tag{88}$$

$$v(t) = (e^{t_f - t} - 1)q_z \quad for \quad t_1 < t \leq t_f \tag{89}$$

To be noted: The authors have only considered functions

$$z(t) = e^{-t}(q_z - v_0) + q_z(t-1) + v_0 \tag{90}$$

and

$$v(t) = (v_0 - q_z)e^{-t} + q_z \tag{91}$$

for calculating position and velocity of the robot, but as per our previous results, they are only in the range $0 < t \leq t_1$ hence we are also considering the equations for $t_1 < t \leq t_f$

7.1 Plotting the trajectory

To be noted: The authors have taken initial conditions as follows,
$x_0 = y_0 = 0m, x_f = y_f = 1m \ v_{x0} = 0.2m/s, v_{y0} = -0.5m/s$

It is obvious that with these initial conditions, the robot is supposed to move in the fourth quadrant of the plane. But from Fig. 7. , we can see that the robot moves in the second quadrant.

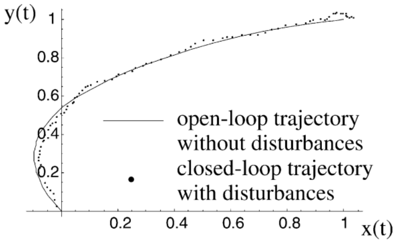

Fig. 7. Simulation with noise.

When we take initial conditions as

$x_0 = y_0 = 0m, \quad x_f = y_f = 1m$
$v_{x0} = -0.5m/s, \quad v_{y0} = 0.2m/s.,$
we get a result similar to that of Fig 7.

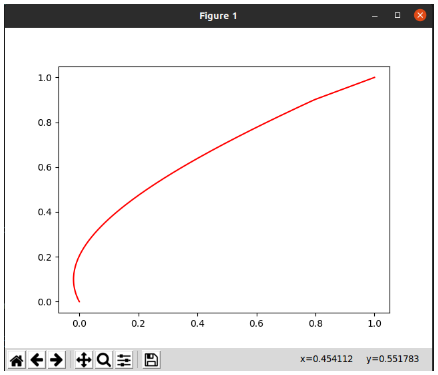

Fig 8. Simulation output of our code

7.2 Plotting the trajectory

As the initial conditions are reversed, the plots are also reversed, i.e. qx of the paper is qy of the code output and vice versa

Output as per the paper:

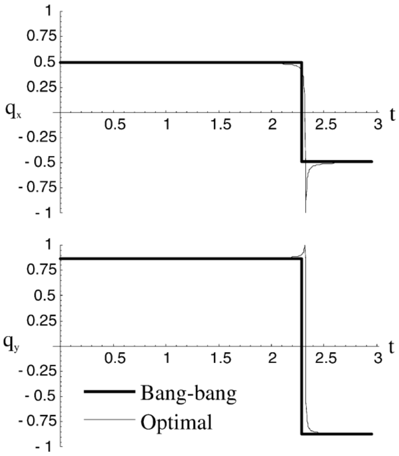

Fig 9. Comparison of optimal and approximate solution from the paper

Outputs as per our code:

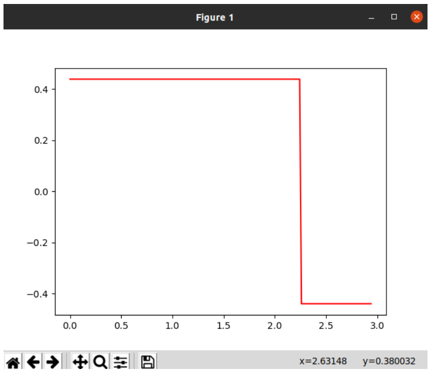

Fig 10. q_x vs t Simulation

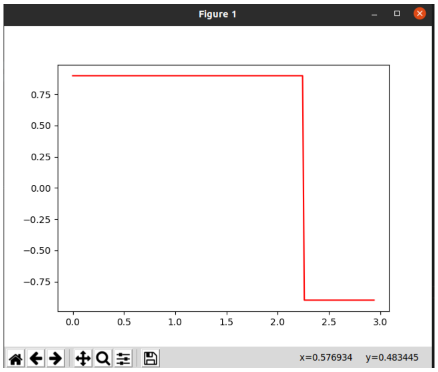

Fig 11. q_y vs t Simulation

8 Conclusion

As translational degrees of freedom of an omnidirectional vehicle can be made independent of its rotational degrees of freedom, restricting admissible control has been used to greatly simplify the complex non linear control problem. The proposed control strategy is very simple yet effective. Even though it does not provide the "optimal" trajectory, it provides a near optimal trajectory, in a much more computationally effective way. Considering the benefits of computational efficiency,the difference in the two trajectories is quite acceptable. Thus the proposed strategy can prove to be useful in many scenarios where low cost of computation is required with a significant tolerance to the output error. For example, this strategy would be very efficient for field mapping applications.

9 Appendix 1:

Fig. 9 shows the cuboid. The radius of the largest contained solid of revolution at a fixed $q\theta$ is simply the radius of the biggest circle that can be inscribed into the polygonal intersection of the cuboid and the plane $q_\theta(t) =$ constant. (Fig. 9 also shows this circle at $q_\theta(t) = 1$.) Because of the symmetry of the cuboid, it is enough to study the plane

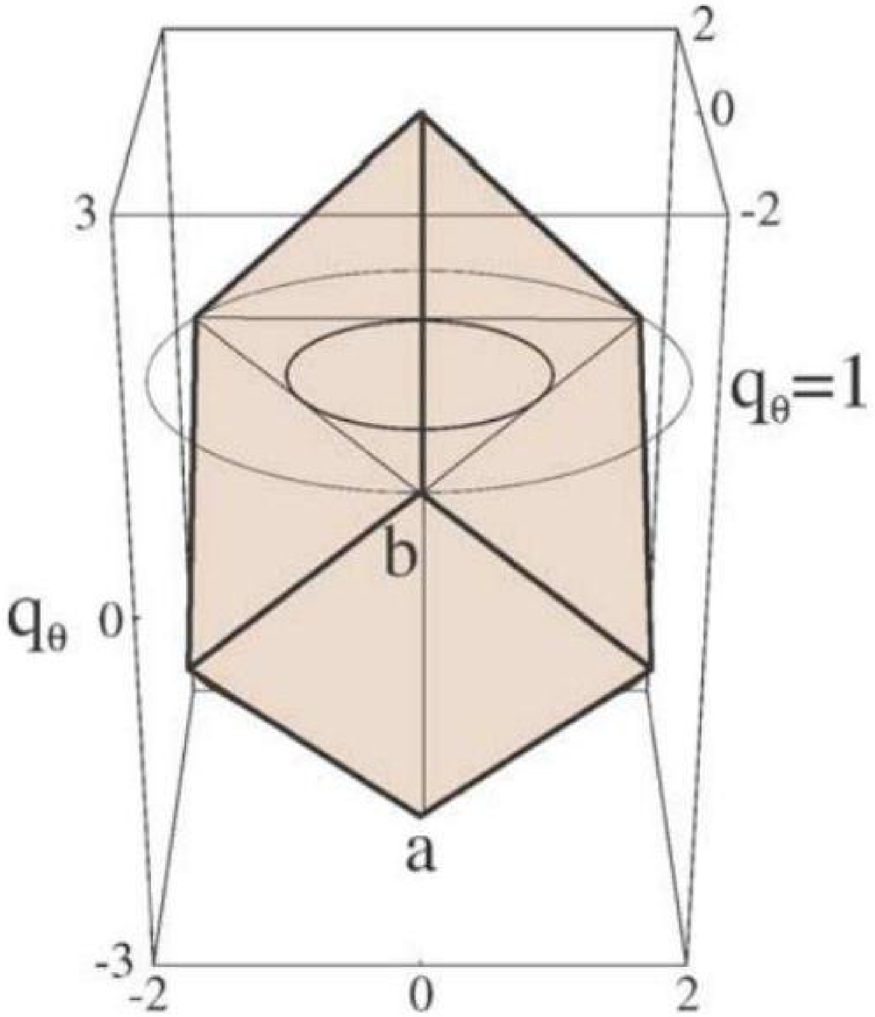

Fig. 9. Geometry of the cuboid.

containing the line segment ab. It is easy to see that the radius sought is just the distance of this line from the q_θ axis at a given height. The segment ab connects point $(0, 0, -3)$ and $(0, -2, 1)$ so its equation is

$$\begin{aligned} \mathrm{q_y(t)} &= \frac{1}{2}\left(3 + \mathrm{q_\theta(t)}\right) \\ \mathrm{q_x(t)} &= 0 \\ -3 \leq \mathrm{q_\theta(t)} &\leq 1 \end{aligned} \tag{92}$$

The solid of revolution is characterized by

$$\mathrm{q_x^2(t)} + \mathrm{q_y^2(t)} \leq \left(\frac{3 - |\mathrm{q_\theta(t)}|}{2}\right)^2 = \mathrm{r^2\left(q_\theta(t)\right)} \tag{93}$$

10 Appendix 2

To prove Proposition 1 we first define

$$w = \frac{1}{2}q.$$

Then t_2 can be expressed as

$$t_2 = \frac{1}{2}t_\mathrm{f} + cw.$$

With (67) and (B.2), Eq. (66) can be recast as

$$\mathrm{e}^{-cw} = \cosh\left(\frac{1}{2}t_\mathrm{f}\right) - v_0\mathrm{e}^{-t_\mathrm{f}/2}w.$$

Fig. 10 shows the left and right hand side of Eq. (B.4) as a function of w for the case of $c > 0$.

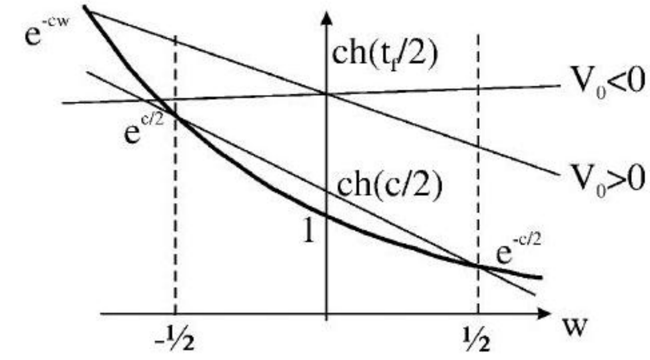

Fig. 10. Solution to the fixed-time problem. Proposition 2. For all $t_\mathrm{f} > t_{\mathrm{f\,min}}$ there exists aw that satisfies

$$\mathrm{e}^{-cw} = \cosh\left(\frac{1}{2}t_\mathrm{f}\right) - v_0\mathrm{e}^{-t_\mathrm{f}/2}w,$$

and $|w| > 1/2$. Further, the execution time t_f is a strictly monotonous function of q with $\lim t_\mathrm{f} \to \infty$ as $q \to 0$.

Proof. First we show that

$$t_{\mathrm{f}} \geq |c|,$$

or equivalently

$$\cosh\left(\frac{1}{2}t_{\mathrm{f}}\right) \geq \cosh\left(\frac{c}{2}\right).$$

To see this, consider the inequalities

$$\begin{aligned} t_{\mathrm{f}} &= t_1 + t_2 \geq t_2, \\ t_1 &= t_2 - \frac{c}{q} \geq 0 \Rightarrow t_2 \geq \frac{c}{q} \end{aligned}$$

if $\operatorname{sgn}(c/q) = 1$

$$\frac{c}{q} = |c| \Rightarrow t_2 \geq |c| \Rightarrow t_{\mathrm{f}} \geq |c|$$

if $\operatorname{sgn}(c/q) = -1$

$$t_{\mathrm{f}} = \ln(1+\sqrt{D})^2 - \frac{c}{q} = \ln(1+\sqrt{D})^2 + |c| \geq |c|$$

since $D \geq 0$.

Using this we are able to show the existence of roots with $|w| > 1/2$.

If $v_0 < 0$ then the slope of the line

$$\cosh\left(\frac{1}{2}t_{\mathrm{f}}\right) - v_0 \mathrm{e}^{-t_{\mathrm{f}}/2} w, \quad t_{\mathrm{f}} > t_{\mathrm{f\ min}}$$

will decrease, so the w coordinate of its intersection with the exponential function will always be less than $-1/2$.

If $v_0 > 0$ then the line (B.11) will have one intersections with the exponential function e^{-cw}, for which

$$w > w^* = \frac{1}{2} \quad \text{or} \quad w < w^* = -\frac{1}{2}.$$

If $\mathrm{e}^{c/2} \leq \cosh(t_{\mathrm{f}}/2)$ then the line (B.11) and e^{-cw} will have one intersection (since the positive slope of the line is decreasing with increasing t_{f}) with

$$w < -\frac{1}{2}.$$

These arguments also shows that increasing $|w|$ corresponds to increasing t_{f} (that is $|w|(|q|)$ is a monotonously increasing (decreasing) function of t_{f}). The converse is also true: t_{f} is a strictly monotonously increasing function of q with $\lim t_{\mathrm{f}} \to \infty$ as $q \to 0$. The $c < 0$ case can similarly be proved. This concludes the proof.

11 References

[1] M. Asada, H. Kitano (Eds.), RoboCup-98: Robot Soccer World Cup II, Lecture Notes in Computer Science, Springer, New York, 1999.

[2] M. Athans, P.L. Falb, Optimal Control: An Introduction to the Theory and its Applications, McGraw-Hill, New York, 1966.

[3] B. d'Andréa-Novel, G. Bastin, G. Campion, Dynamic feedback linearization of nonholonomic wheeled mobile robots, Proceedings of the IEEE International Conference on Robotics and Automation 3 (1992) 2527-2532. [4] R. D'Andrea, T. Kalmár-Nagy, P. Ganguly, M. Babish, The Cornell RoboCup Team, in: G. Kraetzschmar, P. Stone, T. Balch (Eds.), Robot Soccer World Cup IV, Lecture Notes in Artificial Intelligence, Vol. 2019, Springer, Berlin, 2001, pp. 41-51.

[5] D. Balkcom, M. Mason, Time optimal trajectories for bounded velocity differential drive robots, Proceedings of the IEEE International Conference on Robotics and Automation 3 (2000) 2499-2504.

[6] N. Faiz, S.K. Agrawal, Trajectory planning of robots with dynamics and inequalities, Proceedings of the 2000 IEEE International Conference on Robotics and Automation 4 (2000) 3976-3982.

[7] N. Faiz, S.K. Agrawal, R.M. Murray, Trajectory planning of differentially flat systems with dynamics and inequalities, AIAA Journal of Guidance, Control, and Dynamics 24 (2) (2001) 219-227.

[8] P. Fiorini, Z. Shiller, Time optimal trajectory planning in dynamic environments, Journal of Applied Mathematics and Computer Science, Special Issue on Recent Development in Robotics 7 (2) (1997) 101-126.

[9] E. Frazzoli, M.A. Dahleh, E. Feron, Real-time motion planning for agile autonomous vehicles, AIAA Journal of Guidance, Control, and Dynamics 25 (1) (2002) 116-129.

[10] M. Jung, H. Shim, H. Kim, J. Kim, The miniature omni-directional mobile robot OmniKity-I (OK-I), Proceedings of the International Conference on Robotics and Automation 4 (1999) 2686-2691.

[11] H. Kitano, J. Siekmann, J.G. Garbonell (Eds.), RoboCup-97: Robot Soccer World Cup I, Vol. 139, Lecture Notes in Computer Science #1395, Springer, New York, 1998.

[12] K.C. Koh, H.S. Cho, A smooth path tracking algorithm for wheeled mobile robots with dynamic constraints, Journal of Intelligent and Robotic Systems 24 (1999) 367-385.

[13] K.L. Moore, N.S. Flann, Hierarchial task decomposition approach to path planning and control for an omni-directional autonomous mobile robot, Proceedings of the International Symposium on Intelligent Control/Intelligent Systems and Semiotics (1999) 302 – 307.

[14] V. Muñoz, A. Ollero, M. Prado, A. Simón, Mobile robot trajectory planning with dynamics and kinematics constraints, Proceedings of the IEEE International Conference on Robotics and Automation 4 (1994) 2802-2807.

[15] D.A. Pierre, Optimization Theory with Applications, 2nd Ed., Dover, New York, 1986.

[16] F.G. Pin, S.M. Killough, A new family of omnidirectional and holonomic wheeled platforms for mobile robots, IEEE Transactions on Robotics and Automation 10 (4) (1994) 480-489.

[17] M. Renaud, J.Y. Fourquet, Minimum time motion of a mobile robot with two independent, acceleration-driven wheels, in: Proceedings of the 1997 IEEE International Conference on Robotics and Automation, 1997, pp. 2608-2613.

[18] Y. Tanaka, T. Tsuji, M. Kaneko, P.G. Morasso, Trajectory generation using time-scaled artificial potential field, in: Proceedings of the 1998 IEEE/RSJ International Conference on Intelligent Robots and Systems, vol. 1, 1998, pp. 223-228.

[19] M. Veloso, E. Pagello, H. Kitano (Eds.), RoboCup-99: Robot Soccer World Cup III, Lecture Notes in Computer Science, #1856 Springer, New York, 2000.

[20] K. Watanabe, Y. Shiraishi, S.G. Tzafestas, J. Tang, T. Fukuda, Feedback control of an omnidirectional autonomous platform for mobile service robots, Journal of Intelligent and Robotic Systems 22 (3) (1998) 315-330.